Accelerated global warming by metabolic imbalances on Earth

Gesa A. Weyhenmeyer*,[1]

[1]Department of Ecology and Genetics/Limnology, Uppsala University, 75236 Uppsala, Sweden

*Corresponding author: Gesa Weyhenmeyer, Gesa.Weyhenmeyer@ebc.uu.se, phone: +46-768383106

Author contribution statement: GW initiated the project, came up with all concepts, performed all data analyses and wrote the paper.

Key points:

- A temperature departure from solar irradiance co-varies with a long-lasting imbalance between photosynthesis and ecosystem respiration.
- Metabolic imbalances increase under anthropogenic global warming, causing a greenhouse gas and energy accumulation in the atmosphere.
- Earth's warming and cooling events are driven by metabolic imbalances.

Abstract

Global warming is presently accelerating, raising the question whether all climate forcing and feedback mechanisms have been accounted for. Here a metabolic climate forcing and feedback mechanism is introduced, providing an explanation for the observed accelerated global warming. Based on more than 400,000 meteorological observations at various latitudes, it is shown that temperatures at the Earth's surface increasingly depart from thermodynamic equilibrium conditions towards warming at all examined geographical locations because of a long-lasting imbalance between the exothermic metabolic process of ecosystem respiration and the endothermic metabolic process of photosynthesis. Following the principles of the metabolic theory, metabolic imbalances are attributed to warmer temperatures stimulating ecosystem respiration at the same time as photosynthesis becomes light constrained. Since metabolic imbalances are expected to continue until ecosystem respiration becomes substrate limited, there is an urgent need to navigate climate mitigation towards measures that can slow down ecosystem respiration.

1. Introduction

The global carbon cycle plays a key role in regulating Earth's temperature with carbon-climate feedback mechanisms well integrated into Earth System Models (Friedlingstein & Prentice, 2010). By far the largest fluxes in the global carbon cycle comprise photosynthesis and ecosystem respiration (Friedlingstein et al., 2022; Masson-Delmotte et al., 2021). Both fluxes are driven by the metabolic rate of individual organisms on Earth, causing energy and carbon to be frequently exchanged between the atmosphere and the biosphere, thereby influencing Earth's climate (Falkowski et al., 2000). According to the metabolic theory of ecology the ultimate driver for the metabolic rate on Earth is temperature, following the kinetics described by the Van't Hoff-Arrhenius relation (Brown et al., 2004; Gillooly et al., 2001):

$$B_i = b_0 \cdot e^{-E_a/(k_B \cdot T)} \cdot M_i^{\alpha} \quad (1)$$

where B_i is the metabolic rate of any optional organism (measured as energy in watts or as oxygen consumption or carbon dioxide production per unit time), b_0 is a normalization constant independent of body size and temperature, E_a is the average activation energy in eV, k_B is the Boltzmann's constant ($8.62 \cdot 10^{-5} \cdot \mathrm{eV} \cdot \mathrm{K}^{-1}$), T is the absolute temperature in K, M_i is body size expressed as pgC and α is the allometric scaling exponent for body size.

Temperature alone is, however, not the only fundamental physical constraint on the metabolic rate on Earth. Photoautotrophs can, for example, only survive when they receive sufficient energy from the sun (Relyea, 2021). To account for the dependency of the photosynthetic rate on light, Lopez-Urrutia et al. (2006) extended the metabolic theory of ecology by the Michaelis-Menten photosynthetic light response:

$$P_i = p_0 \cdot e^{-E_a/(k_B \cdot T)} \cdot M_i^{\alpha} \cdot \left(\frac{PAR}{k_m + PAR}\right) \quad (2)$$

where P_i is the rate of individual gross photosynthesis in mmol of $O_2 \cdot d^{-1}$, p_0 is a normalization constant independent of body size, temperature and light, E_a is the average activation energy for photosynthetic reactions in eV, k_B is the Boltzmann's constant ($8.62 \cdot 10^{-5} \cdot eV \cdot K^{-1}$), T is the absolute temperature in K, M_i is body size expressed as pgC, α is the allometric scaling exponent for autotroph body size, PAR is the daily irradiance in mol photons$\cdot m^{-2} \cdot d^{-1}$ and k_m is the Michaelis-Menten half-saturation constant in mol photons$\cdot m^{-2} \cdot d^{-1}$.

According to the extended metabolic theory, eq. 1 is applicable for the prediction of the heterotrophic respiration rate while eq. 2 needs to be applied for the prediction of the photosynthetic rate. Both rates are presently assumed to be in balance over the course of a year and on the global scale, as, for example, illustrated in the annually renewed global carbon budget (Friedlingstein et al., 2022; Friedlingstein et al., 2020). During a 24-hour period, it is, however, well known that the rates are commonly out of balance with either photosynthesis or ecosystem respiration dominating, depending on the availability of sunlight (Wilson et al., 2002). In some ecosystems, respiration can even exceed photosynthesis over several years, as shown for lake ecosystems in the boreal region (Cole et al., 1994; Drake et al., 2018; Raymond et al., 2013; Tranvik et al., 2009). In those ecosystems, the heterotrophic respiration flux is disproportionally large due to the availability of inflowing organic carbon as an extra, light-independent energy source, which microorganisms are capable to efficiently utilize (Cole et al., 1994). Such long-lasting metabolic imbalances with a clear dominance of the exothermic process of ecosystem respiration are expected to cause a substantial greenhouse gas and temperature increase in the atmospheric boundary layer, further accelerating the global warming trend.

Presently, it is not known where, when and for how long metabolic imbalances on Earth occur and how temperatures at the Earth's surface are related to such imbalances. An imbalance

between the endothermic process of photosynthesis and the exothermic process of ecosystem respiration corresponds to non-equilibrium conditions at the Earth's surface. Under such conditions, not only photosynthesis (*P*) and ecosystem respiration *(ER)* are out of balance but also Earth's absorptivity *(α)* and emissivity *(ε)*. A comparison between the *P/ER* and the *α/ε* ratio is relevant for the understanding of Earth's temperature for various reasons. Both ratios describe how light reaching the Earth's surface can finally be transformed to heat. Under thermodynamic equilibrium conditions, the light-to-heat ratio at the Earth's surface follows the principles of the Stefan-Boltzmann law, and all ratios receive a value of one (Fig. 1):

$$\overbrace{\frac{P}{ER}}^{Earth's\ metabolism} = \overbrace{\frac{\alpha}{\varepsilon}}^{Kirchhoff's\ law} = \overbrace{\frac{G_s}{T_S^4 \cdot \sigma}}^{Stefan-Boltzmann\ law} = 1 \qquad (3)$$

where *P* is the photosynthetic rate in W, *ER* is the ecosystem respiration rate in W, α is the absorptivity of the Earth's surface, ε is the emissivity of the Earth's surface, G_s is the solar irradiance at the Earth's surface in $W \cdot m^{-2}$, T_s is the absolute temperature at the Earth's surface in K and σ is the Stefan-Boltzmann constant in $W \cdot m^{-2} \cdot K^{-4}$.

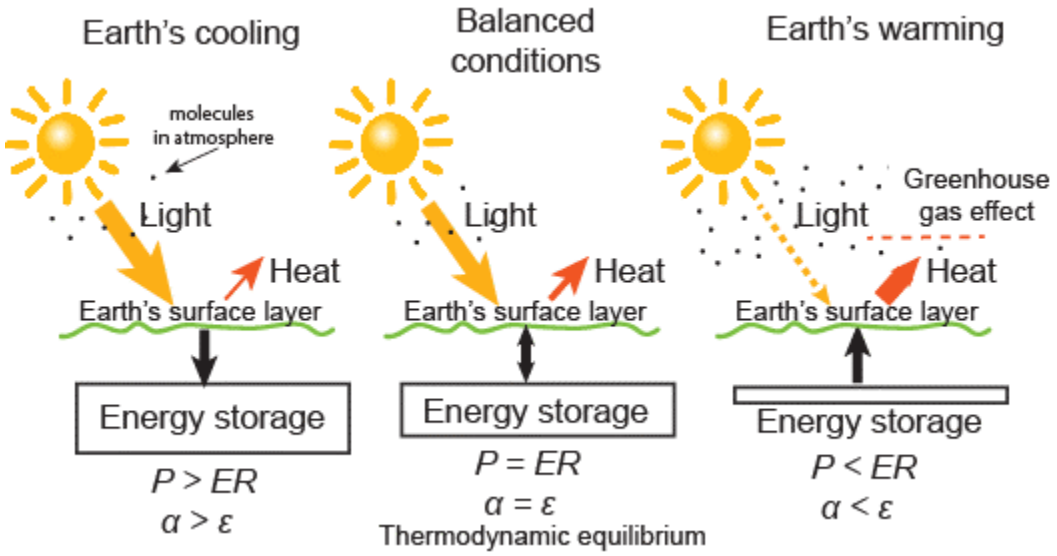

Figure 1. Concept of Earth's cooling and warming. Whenever sufficient light reaches the Earth's surface, photosynthesis (*P*) commonly exceeds ecosystem respiration (*ER*) and absorptivity (α) exceeds emissivity (ε). Under such conditions energy is stored in the Earth's surface layer in form of heat and organic carbon. When solar irradiance decreases to critical low values, *P* and α become light constraint. Under those conditions, *ER* becomes larger than *P* and α larger than ε, implying that the stored energy in the Earth's surface layer is consumed and released into the atmospheric boundary layer with a consequent warming effect.

With decreasing light reaching the Earth's surface, which is not only driven by the solar cycle but also strongly by the amount and characteristics of molecules in the atmosphere (Lacis et al., 1981; Masson-Delmotte et al., 2021), *P* and α can become light constraint. Under light limitation the exothermic process of ecosystem respiration as well as the emission of heat from the Earth's surface can potentially continue until all stored energy in form of heat or organic carbon in the Earth's surface layer is depleted, resulting in a net heat and greenhouse gas flux from the Earth's surface into the atmosphere, with a consequent warming of the atmospheric boundary layer (Fig. 1).

Assuming that light-to-heat transformation processes at the Earth's surface such as photosynthesis and ecosystem respiration as well as Earth's absorptivity and emissivity co-vary due to their direct dependency on the solar cycle, it is hypothesized that variations in those processes determine in how far temperature departs from thermodynamic equilibrium conditions and the principles of the Stefan-Boltzmann law as follows:

$$\overbrace{\frac{\hat{P}}{ER}}^{Earth's\ metabolism} = \overbrace{\frac{G_S}{T_S^4 \cdot \sigma}}^{Solar\ irradiance-temperature\ relation} \quad (4)$$

where *P* is the photosynthetic rate in W, *ER* is the ecosystem respiration rate in W, G_s is the solar irradiance at the Earth's surface in $W \cdot m^{-2}$, T_s is the absolute temperature at the Earth's surface in K and σ is the Stefan-Boltzmann constant in $W \cdot m^{-2} \cdot K^{-4}$.

To test the hypothesis more than 400,000 meteorological observations at the Earth's surface at various latitudes were used, where the *P/ER* ratio was determined by applying the main principles of the extended metabolic theory of ecology.

2. Methods

2.1. Identification of metabolic imbalances

The balance between *P* and *ER* is, according to the extended theory by Lopez-Urrutia et al., (2006), a direct function of the Michaelis-Menten photosynthetic light response, or in a wider sense, a direct function of solar irradiance. The *P/ER* ratio is here seen as a reversible chemical

reaction at the Earth's surface which goes into the direction of the endothermic process of *P* with values above one when solar irradiance exceeds an equilibrium constant or into the direction of the exothermic process of *ER* with values less than one when solar irradiance is smaller than the equilibrium constant. Thus, based on metabolic theory and basic chemistry, the *P/ER* ratio is here expressed as:

$$\frac{P}{ER} = \frac{Gs}{k_{eq}} \quad (5)$$

where *P* is the photosynthetic rate in W, *ER* is the ecosystem respiration rate in W, G_s is the solar irradiance at the Earth's surface in $W \cdot m^{-2}$ and k_{eq} is the thermodynamic equilibrium constant in $W \cdot m^{-2}$.

With a known thermodynamic equilibrium constant and available solar irradiance data eq. 5 allows to determine metabolic imbalances at any particular location and any particular time in the world. Although the determination of metabolic imbalances at a particular time of the year might be of interest, it is rather the identification of long-term metabolic imbalances which provides most value for the understanding of global warming. For such an identification, the data distribution over an entire year needs to be considered, which in this study corresponded to an evaluation of annual mean values of $\left(\frac{Gs}{k_{eq}}\right)$.

2.2. Data material and analyses

Metabolic imbalances as well as temperature departures from thermodynamic equilibrium conditions were examined by using hourly solar irradiance and air temperature data from the Swedish Meteorological and Hydrological Institute (SMHI) and the National Aeronautics and Space Administration (NASA). The examination began with observational data from SMHI, for which three locations were chosen, representing a large range of latitudes: Kiruna in the North of Sweden (decimal degrees: 67.83 N, 20.34 E; altitude: 459 m; station number: 180940), Östersund in the central part of Sweden (decimal degrees: 63.20 N and 14.49 E; altitude: 356 m; station number: 134110) and Växjö in the southern part of Sweden (decimal degrees: 56.85 N and 14.83 E; altitude: 199 m; station number: 64510). Hourly air temperature data for these locations, measured 2 m above ground, were downloaded from: https://www.smhi.se/data/meteorologi/ladda-ner-meteorologiska-

observationer/#param=airtemperatureInstant,stations=all. To get homogenous datasets, data were taken from 2008 to 2021 (January 1 to December 31). All data were quality checked by SMHI. In addition to observational air temperature data, observational global irradiance data in $W \cdot m^{-2}$ were downloaded for the three locations from: https://www.smhi.se/data/meteorologi/ladda-ner-meteorologiska-observationer/#param=globalIrradians,stations=all. Measurements were performed using a pyranometer. All irradiance data were quality checked by SMHI. In total 367,917 quality checked hourly air temperature and global irradiance observational data were available and used in this study.

The results from Sweden were then validated with data from North America, available as gridded data from https://power.larc.nasa.gov/data-access-viewer/. The downloaded data represented a wide variety of landscapes and latitudes with one randomly chosen site located in Texas, one in the Appalachian Mountains in Pennsylvania and one in northern Ontario. For parameter description and methodology of the data from North America it is referred to the description by NASA at https://power.larc.nasa.gov/data-access-viewer/. From North America, altogether 52,614 hourly data during 2020-2021 (January 1 to December 31) were downloaded.

All data analyses were performed in JMP, version 15.2.0., SAS Institute Inc.

3. Results

3.1. Metabolic imbalances and temperature departures from thermodynamic equilibrium conditions

Using more than 300,000 hourly solar irradiance and air temperature observations along a latitudinal gradient in Sweden, a 1:1 relationship between the *P/ER* ratio, expressed by applying eq. 5, and a temperature departure from thermodynamic dynamic equilibrium conditions and the principles of the Stefan-Boltzmann law as outlined in eq. 4 was achieved by choosing a thermodynamic equilibrium constant of 359 $W \cdot m^{-2}$. Due to residuals being strongly skewed a natural logarithmic relationship was applied, giving a R^2 value of 0.998, an intercept close to zero and a slope of 0.98 (Fig. 2a). Validation with more than 52,000 hourly meteorological data from North America and using the same value for the equilibrium constant, i.e. 359 $W \cdot m^{-2}$, confirmed a direct interaction between Earth's metabolism and the Earth's climate system as described by

eq. 4 (Fig. 2b). Changing the value of k_{eq} neither changed the predictive power of the model nor the value of the slope but caused the intercept to increasingly deviate from zero. A k_{eq} value of 359 $W \cdot m^{-2}$ resulted in the smallest intercept at all meteorological sites and during all years. However, despite intercepts very close to zero there were slight variations in the intercept among years and among sites, implying small variations in the equilibrium constant. Variations in k_{eq} can be a consequence of stressed equilibrium conditions, which according to the Le Châtelier's principle can cause shifts in equilibrium conditions.

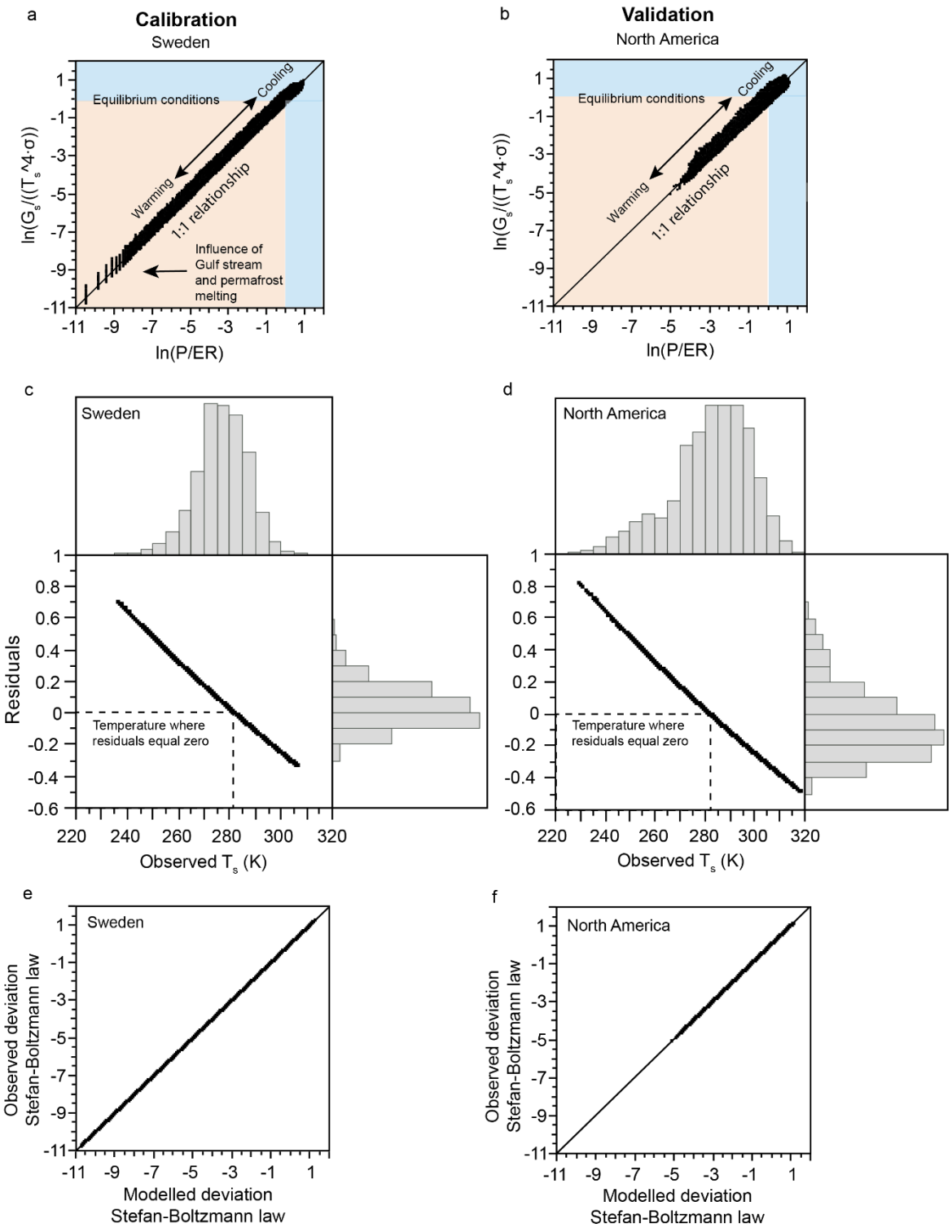

207

208 **Figure 2. Variations in hourly light-temperature relations at six sites with contrasting land-cover in**
209 **relation to metabolic imbalances (Sweden: Kiruna, Östersund, Växjö; North America: Ontario,**
210 **Pennsylvania, Texas).** Light-temperature relations are based on the Stefan-Boltzmann law ($G_s/T_s^4\sigma$ where

211 G_s is the solar irradiance at the Earth's surface in $W \cdot m^{-2}$, T_s is the absolute temperature at the Earth's surface
212 in K, σ is the Stefan-Boltzmann constant in $W \cdot m^{-2} \cdot K^{-4}$) and metabolic imbalances are expressed as the ratio
213 between photosynthesis (P) and ecosystem respiration (ER), modelled as a function of solar irradiance (see
214 eq. 5). (**a), (b).** Linear relationships between modelled metabolism and observed light-temperature relations
215 at the Earth's surface (R^2 = 0.998, p < 0.0001 for Sweden, for which the model was calibrated and R^2 =
216 0.970, p < 0.0001 for North America, for which the model was validated). Whenever there was a metabolic
217 imbalance ($P>ER$ and $P<ER$, respectively), the light-temperature relation deviated from the Stefan
218 Boltzmann law. Equilibrium conditions, where P equaled ER, were reached at 359 $W \cdot m^{-2}$. **(c), (d)** Model
219 residuals from panels a and b, respectively, in relation to observed temperatures at the Earth's surface. (**e),**
220 **(f)** Final metabolic-theory based climate forcing and feedback model where results from panels a to d were
221 combined (see eq. 4 for exact model description).

222 Although the prediction of a temperature departure from thermodynamic equilibrium conditions
223 at the Earth's surface was powerful with R^2 values ranging between 0.966 and 0.998 at sites with
224 highly varying land cover across Sweden and North America (Fig. 2a-b), there were deviations
225 from a perfect 1:1 relationship. The residuals from a 1:1 relationship shifted from being positive
226 to becoming negative, showing a perfect inverse relationship to temperature (Fig. 2c-d). A perfect
227 inverse relationship to temperature is an indication of a temperature induced increase in kinetic
228 energy, which is supported by the fact that the residuals could to 100 % be described by applying
229 the concept of the Boltzmann factor (1:1 relationship with an R^2 value of 1):

230 $$Model\ residuals = ln\left(\left(\frac{E_a}{k_B \cdot T_S}\right)^4\right) = ln\left(\left(\frac{T_0}{T_S}\right)^4\right) \quad (6)$$

231 where E_a is the activation energy, here with a value of 0.024 eV, k_B is the Boltzmann's constant
232 ($8.62 \cdot 10^{-5} \cdot eV \cdot K^{-1}$), T_s is the absolute temperature at the Earth's surface in K, and T_o is the
233 temperature when model residuals equaled zero which was the case at 282 K (Fig. 2c-d). In the
234 equation the natural logarithm was used since model residuals were given as logarithmic values.
235 In addition, the fourth power of temperature was used, which is a result of the model structure,
236 where the Stefan-Boltzmann law has been applied.
237
238 Combining all results gave a full explanation of observed solar irradiance-temperature relations
239 at the Earth's surface at any particular location and any particular time by consideration of
240 metabolic processes (1:1 relationship with an R^2 value of 1; Fig. 2e-f):

$$\overbrace{ln\left(\frac{G_S}{T_S^4 \cdot \sigma}\right)}^{Observed} = \overbrace{ln\left(\frac{Gs}{k_{eq}}\right)}^{Climate\ forcing} + \overbrace{ln\left(\left(\frac{T_o}{T_S}\right)^4\right)}^{Feedback} \quad (7)$$

where G_s is the solar irradiance at the Earth's surface in $W \cdot m^{-2}$, T_s is the absolute temperature at the Earth's surface in K, σ is the Stefan-Boltzmann constant in $W \cdot m^{-2} \cdot K^{-4}$, k_{eq} is the equilibrium constant for processes at the Earth's surface in $W \cdot m^{-2}$ corresponding to 359 $W \cdot m^{-2}$, T_o is the temperature when the temperature feedback equaled zero which was the case at 282 K.

3.2. Occurrence of long-lasting metabolic imbalances

For the determination of long-lasting metabolic imbalances annual-mean values of $ln\left(\frac{Gs}{k_{eq}}\right)$ were analyzed. The use of the logarithm resulted from the best model performance (eq. 7), where values larger or smaller than zero were considered as metabolic imbalances. The use of the logarithm implied that conditions during complete darkness were neglected which from a theoretical point of view is logical as there would not be any absorptivity and photosynthesis during complete darkness. However, if darkness persists only for a short time, ecosystem respiration and heat emission can still be ongoing until the energy storage in the Earth's surface layer is depleted. Thus, in this study estimates of long-lasting metabolic imbalances are rather under- than overestimated. Nevertheless, annual-mean values of $ln\left(\frac{Gs}{k_{eq}}\right)$ at all examined sites and for all examined years remained always less than zero, reflecting a long-lasting imbalance between photosynthesis and ecosystem respiration. The lowest annual-mean values, ranging between -2.19 and -2.47, were all observed in Kiruna in northern Sweden. Kiruna is located in a geographical region with access to a large amount of light-independent energy, i.e. at this location extra heat is received from the Gulf Stream (Oort, 1964), and permafrost melting gives access to a large amount of organic carbon, stimulating the exothermic process of ecosystem respiration (Schuur et al., 2015).

4. Discussion

The results of this study support the hypothesis that Earth's metabolism directly interacts with the Earth's climate system where a 1:1 relationship between the *P/ER* ratio and the solar

irradiance-temperature relation at the Earth's surface could be established (Fig. 2). The main findings are based on the extended metabolic theory of ecology, which states that the ultimate drivers of the metabolic rate on Earth are sunlight and temperature (Lopez-Urrutia et al., 2006). Thus, whenever sunlight and temperature are in balance, following the principles of the Stefan Boltzmann law, also photosynthesis and ecosystem respiration are in balance.

At present, temperatures are, however, not any longer in balance with solar irradiance, as there were substantial long-term temperature departures from thermodynamic equilibrium conditions towards warming (Fig. 2a-b). The ongoing temperature departure from thermodynamic equilibrium conditions is well known as the greenhouse gas driven global warming trend (Masson-Delmotte et al., 2021). When temperature on Earth increases, also metabolic rates on Earth increase according to the metabolic theory of ecology (Brown et al., 2004; Schramski et al., 2015). Despite a stimulation of both the photosynthetic and the respiration rate by increasing temperature, globally also seen in an overall greening trend of the Arctic under global warming (Myers-Smith et al., 2020), ecosystem respiration can profit more from a temperature increase due to a light constrain on photosynthesis during many hours of a year. Thus, there is a threshold when the photosynthetic rate switches from being temperature to becoming light constrained (Fig. 3). Under light constrains which here were identified to begin when solar irradiance is less than 359 $W \cdot m^{-2}$, ecosystem respiration exceeds photosynthesis, causing a net energy and greenhouse gas flux from the biosphere into the atmosphere, further accelerating global warming. The worst-case scenario for accelerated global warming is the combination of low light and high temperature. Under such conditions organic carbon will rapidly be consumed with further greenhouse gas accumulation in the atmosphere, further accelerating warming. The concept of higher reaction rates with increasing temperature is here defined as the climate feedback mechanism (Fig. 3). The concept is supported by a modelling approach showing that carbon turnover rates in ecosystems substantially increase in a warmer climate (Carvalhais et al., 2014). A higher reaction rate can put a lot of pressure on equilibrium conditions, suggesting that the equilibrium constant k_{eq} might be subjected to small changes, following the Le Châtelier's principle.

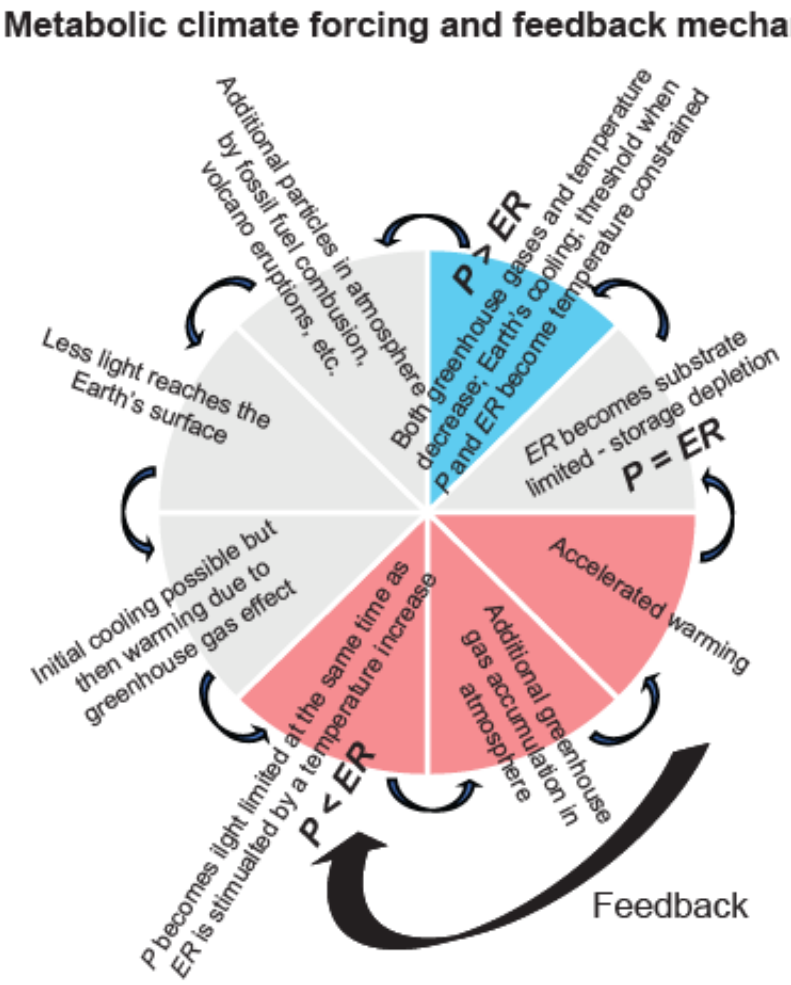

298

299 **Figure. 3. Principles of the Earth's climate system, here introduced as the metabolic climate forcing**
300 **and feedback mechanism.** Because of a greenhouse gas effect, heat is accumulated in the atmospheric
301 boundary layer which stimulates the ecosystem respiration rate more than the photosynthetic rate, due to
302 a fundamental light constrain on photosynthesis. A faster ecosystem respiration rate causes an increased
303 greenhouse gas accumulation in the atmosphere, with a consequent accelerated warming, which gives a
304 climate feedback. The red color indicates the present accelerated global warming trend whereas the blue
305 color indicates cooling events in Earth's history, including ice ages when both photosynthesis and
306 ecosystem respiration become temperature constrained. The metabolic climate forcing and feedback
307 mechanism demonstrates that Earth's cooling and warming events are driven by a switch in the main
308 constraints on Earth's metabolism: when Earth's cools temperature is the main constrain, when Earth's
309 warms light is the main constrain. A switch between warming and cooling events is caused by substrate
310 limitation for ecosystem respiration and a switch between cooling and warming by additional particles
311 and greenhouse gases in the atmosphere from e.g. volcano eruptions and fossil fuel combustion.

Unless there will be a substantial increase in light reaching the Earth's surface, which is unlikely to happen in near future, in particular when taking the strong water vapor climate feedback mechanism into account (Held & Soden, 2000), the large amounts of available light-independent energy resources stored in the Earth's surface layer will make it difficult to turn around the ongoing warming trend. Reversing the general long-lasting warming trend before there is a depletion of the stored energy in the Earth's surface becomes even more difficult considering that a dominance of ecosystem respiration causes a continued greenhouse gas accumulation in the atmosphere, keeping the process of global warming alive. Support for the existence of long-lasting metabolic imbalances in Earth's history is given by a recent study of Jian et al. (2022) who found historically inconsistent productivity and respiration fluxes in the terrestrial global carbon cycle. Also Yvon-Durocher et al. (2010) described a metabolic imbalance with warming, based on experimental aquatic mesocosm work. In addition, the observed changes in the annual carbon dioxide concentration amplitude in the atmosphere (Forkel et al., 2016; Wu & Lynch, 2000) are a clear indication of a change in the *P/ER* ratio although it remains open whether it is photosynthesis exceeding ecosystem respiration as previously suggested or whether it is ecosystem respiration which exceeds photosynthesis. According to the results of this study it is the ecosystem respiration which exceeds photosynthesis.

A direct interaction between Earth's metabolism and Earth's climate, here introduced as the metabolic climate forcing and feedback mechanism (Fig. 3), has been considered previously but Earth System Models and the global carbon budget still assume that photosynthesis and ecosystem are balanced over the course of a year. Since we presently observe long-lasting non-equilibrium conditions with a shift towards the exothermic process of ecosystem respiration climate change studies need to consider thermodynamic non-equilibrium conditions. Here, it was clearly shown that we presently experience widespread metabolic imbalances on Earth with an accelerated temperature increase as a consequence. To counteract ongoing metabolic imbalances ecosystem respiration needs to be slowed down, in particular in the regions where ecosystem respiration exceeds photosynthesis the most. The approach in this study allows to easily identify regions and the kind of land-use where metabolic imbalances are most pronounced. Developing and performing climate mitigation strategies for those regions will help to decrease the ongoing net energy and greenhouse gas flux from the biosphere to the atmosphere.

Acknowledgements

This work has partly been financed by the Swedish Research Council (VR; Grant No. 2020-03222) and the Swedish Research Council for Environment, Agricultural Sciences and Spatial Planning (FORMAS; Grant No. 2020-01091). Many thanks go to panel members of the ERC-Advanced Grant and to students asking all kind of challenging questions, to the Bergman Estate on Fårö Foundation for funding a retreat for manuscript preparation and to James H. Brown and a large number of colleagues for stimulating conversations concerning the metabolic theory of ecology.

Data Availability Statement: All data used in this study are downloaded from public, permanent sources, such as the Swedish Meteorological and Hydrological Institute (https://www.smhi.se/data/meteorologi/ladda-ner-meteorologiska-observationer) and NASA (https://power.larc.nasa.gov/data-access-viewer/). The downloaded data used for model calibration and validation and presented in figure 2 are available as supplementary material.

References

Brown, J. H., Gillooly, J. F., Allen, A. P., Savage, V. M., & West, G. B. (2004). Toward a metabolic theory of ecology. *Ecology, 85*(7), 1771-1789. <Go to ISI>://WOS:000223113500001

Carvalhais, N., Forkel, M., Khomik, M., Bellarby, J., Jung, M., Migliavacca, M., et al. (2014). Global covariation of carbon turnover times with climate in terrestrial ecosystems. *Nature, 514*(7521), 213-+. <Go to ISI>://WOS:000342663100039

Cole, J. J., Caraco, N. F., Kling, G. W., & Kratz, T. K. (1994). Carbon-dioxide supersaturation in the surface waters of lakes. *Science, 265*(5178), 1568-1570. <Go to ISI>://A1994PF33600031

Drake, T. W., Raymond, P. A., & Spencer, R. G. M. (2018). Terrestrial carbon inputs to inland waters: A current synthesis of estimates and uncertainty. *Limnology and Oceanography Letters, 3*(3), 132-142. https://aslopubs.onlinelibrary.wiley.com/doi/abs/10.1002/lol2.10055

Falkowski, P., Scholes, R. J., Boyle, E., Canadell, J., Canfield, D., Elser, J., et al. (2000). The global carbon cycle: A test of our knowledge of earth as a system. *Science, 290*(5490), 291-296. Review. <Go to ISI>://WOS:000089818100034

Forkel, M., Carvalhais, N., Rodenbeck, C., Keeling, R., Heimann, M., Thonicke, K., et al. (2016). Enhanced seasonal CO2 exchange caused by amplified plant productivity in northern ecosystems. *Science, 351*(6274), 696-699. <Go to ISI>://WOS:000369810000037

Friedlingstein, P., Jones, M. W., O'Sullivan, M., Andrew, R. M., Bakker, D. C. E., Hauck, J., et al. (2022). Global Carbon Budget 2021. *Earth System Science Data, 14*(4), 1917-2005. <Go to ISI>://WOS:000787247700001

Friedlingstein, P., O'Sullivan, M., Jones, M. W., Andrew, R. M., Hauck, J., Olsen, A., et al. (2020). Global Carbon Budget 2020. *Earth System Science Data, 12*(4), 3269-3340. <Go to ISI>://WOS:000599511400001

Friedlingstein, P., & Prentice, I. C. (2010). Carbon-climate feedbacks: a review of model and observation based estimates. *Current Opinion in Environmental Sustainability, 2*(4), 251-257. <Go to ISI>://WOS:000283805300008

Gillooly, J. F., Brown, J. H., West, G. B., Savage, V. M., & Charnov, E. L. (2001). Effects of size and temperature on metabolic rate. *Science, 293*(5538), 2248-2251. <Go to ISI>://WOS:000171139400042

Held, I. M., & Soden, B. J. (2000). Water vapor feedback and global warming. *Annual Review of Energy and the Environment, 25*, 441-475. <Go to ISI>://WOS:000166624500014

Jian, J., Bailey, V., Dorheim, K., Konings, A. G., Hao, D., Shiklomanov, A. N., et al. (2022). Historically inconsistent productivity and respiration fluxes in the global terrestrial carbon cycle. *Nature Communications*.

Lacis, A., Hansen, J., Lee, P., Mitchell, T., & Lebedeff, S. (1981). Greenhouse-effect of trace gases, 1970-1980. *Geophysical Research Letters, 8*(10), 1035-1038. <Go to ISI>://WOS:A1981MN15000003

Lopez-Urrutia, A., San Martin, E., Harris, R. P., & Irigoien, X. (2006). Scaling the metabolic balance of the oceans. *Proceedings of the National Academy of Sciences of the United States of America, 103*(23), 8739-8744. <Go to ISI>://WOS:000238278400030

Masson-Delmotte, V., Zhai, P., Pirani, A., Connors, S. L., Péan, C., Berger, S., et al. (2021). *IPCC, 2021: Climate Change 2021: The Physical Science Basis. Contribution of Working Group I to the Sixth Assessment Report of the Intergovernmental Panel on Climate Change*. Cambridge, United Kingdom and New York, NY, USA: Cambridge University Press.

Myers-Smith, I. H., Kerby, J. T., Phoenix, G. K., Bjerke, J. W., Epstein, H. E., Assmann, J. J., et al. (2020). Complexity revealed in the greening of the Arctic. *Nature Climate Change, 10*(2), 106-117. <Go to ISI>://WOS:000512150200006

Oort, A. H. (1964). Computations of the eddy heat and density transports across the Gulf stream. *Tellus, 16*(1), 55-63. <Go to ISI>://WOS:A1964XF68600008

Raymond, P. A., Hartmann, J., Lauerwald, R., Sobek, S., McDonald, C., Hoover, M., et al. (2013). Global carbon dioxide emissions from inland waters. *Nature, 503*(7476), 355-359. <Go to ISI>://WOS:000327163200032

Relyea, R. (2021). *Ecology - The Economy of Nature*. New York, USA: Macmillan Leraning.

Schramski, J. R., Dell, A. I., Grady, J. M., Sibly, R. M., & Brown, J. H. (2015). Metabolic theory predicts whole-ecosystem properties. *Proceedings of the National Academy of Sciences of the United States of America, 112*(8), 2617-2622. <Go to ISI>://WOS:000349911700076

Schuur, E. A. G., McGuire, A. D., Schadel, C., Grosse, G., Harden, J. W., Hayes, D. J., et al. (2015). Climate change and the permafrost carbon feedback. *Nature, 520*(7546), 171-179. <Go to ISI>://WOS:000352454600029

Tranvik, L. J., Downing, J. A., Cotner, J. B., Loiselle, S. A., Striegl, R. G., Ballatore, T. J., et al. (2009). Lakes and reservoirs as regulators of carbon cycling and climate. *Limnology and Oceanography, 54*(6), 2298-2314. <Go to ISI>://000272785700003

Wilson, K., Goldstein, A., Falge, E., Aubinet, M., Baldocchi, D., Berbigier, P., et al. (2002). Energy balance closure at FLUXNET sites. *Agricultural and Forest Meteorology, 113*(1-4), 223-243. <Go to ISI>://WOS:000179188300012

Wu, W. L., & Lynch, A. H. (2000). Response of the seasonal carbon cycle in high latitudes to climate anomalies. *Journal of Geophysical Research-Atmospheres, 105*(D18), 22897-22908. <Go to ISI>://WOS:000089598000016

Yvon-Durocher, G., Jones, J. I., Trimmer, M., Woodward, G., & Montoya, J. M. (2010). Warming alters the metabolic balance of ecosystems. *Philosophical Transactions of the Royal Society B-Biological Sciences, 365*(1549), 2117-2126. <Go to ISI>://WOS:000278163800012